NCAR SPolKa dual-wavelength polarimetric radar: design and improvement of Ka-band radar

Pei-Sang Tsai,*E. Loew, J. Vivekananadan, J. Emmett, C. Burghart, M. Dixon and S. Ellis
Earth Observing Laboratory, National Center for Atmospheric Research, Boulder, Colorado

1. Introduction

Ellis and Vivekanandan et al (2005) demonstrated a technique for water vapor retrieval using dual-wavelength polarimetic radars in Rain in Cumulus over the Ocean (RICO) experiment using the measurements from NCAR dual-wavelength S- and Ka-band radar (S-PolKa). However the Ka-band radar system was operated frugally as the system was not robust enough as the transmitter was not suitable for extended field operation. During the RICO a number of instabilities in the Ka-band radar system were identified. Recently significant upgrades to Ka-band radar system were made for improving the operational lifetime, stability, and sensitivity of the receiver. This paper describes the upgrades to the data processor, transmitter, front-end radio frequency unit.

2. System Upgrades

Farquharson et al. (2005) identified sources of Ka-band instability based on its performance during the RICO deployment. Short lifetime of the magnetron tube, mechanical stress on front-end cables, lack of real-time monitoring capability and errors in the radar data acquisition system caused sub-standard performance of the radar. All of these issues were addressed in 2010 in preparation for the Dynamics of the Madden-Julian Oscillation (DYNAMO) deployment.

Figure 2 shows a simplified block diagram of the upgraded Ka-band radar system. The system uses a three-stage, super-heterodyne configuration. The magnetron transmitter generates 50 kW peak power at 34.693 GHz. The transmitted pulse is coupled through an identical receive channel for coherent-on-receive. A test target pulse is generated by oscillator 1 at 132.5 MHz and it is injected into the receiver as a reference signal. There are four tunable oscillators in the receiver enclosure. They are phase referenced to a 100 MHz PLO, which is then locked to the 10 MHz master GPS STALO. The GPS STALO provides simultaneous time reference for the S-Pol and Ka systems for synchronizing radar transmissions. The received signal goes through three frequency mixing stages, controlled by the Automatic Frequency Control (AFC), and is down-converted to the final intermediate frequency (IF) at 25 MHz.

The AFC is designed to accommodate the frequency drifting of the magnetron transmitter. The AFC estimates the magnetron transmit frequency and then programs all three oscillators in the receiver chain. By constantly analyzing the transmit signal frequency and adjusting oscillator frequencies, it ensures the received signal lies at the center of receiver passband.

The transmitter was replaced with CPI SFD-319 magnetron. The manufacturer specifies an operating life span of 10,000 hours. It has less frequent arcing and better pulse shape than the original Litton L-4064A magnetron. The peak output power of the transmitter is 76.99 dBm, measured at its detected RF port. The SFD-319 is frequency-tunable. This capability enables VSWR optimization between the antenna and transmitter. The data acquisition computer was upgraded to a Linux-based platform with a Pentek 100 MS/s, 14-bit, commercial, off-the-shelf digital receiver. Firmware for the digital down-conversion was developed in house and it currently being used on several platforms. This technology is a great

*Pei-Sang Tsai, NCAR/EOL P.O. Box 3000, Boulder CO 80301. E-mail: ptsai@ucar.edu,

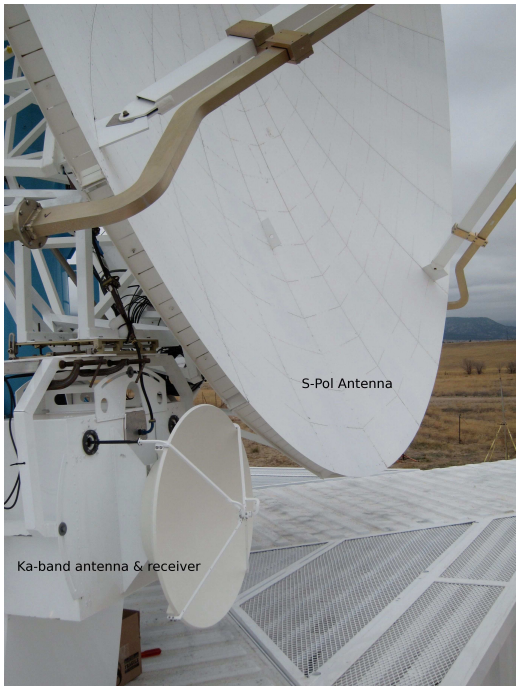

Figure 1: NCAR S-PolKa dual-wavelength radar system. Ka-band radar is attached to the bottom of S-band parabolic antenna. Antenna diameter for S- and Ka-band are 8.5 m and 0.7 m.

improvement over its predecessor; the 20 MS/s, 12-bit resolution Sampler Card used in RICO 2004. In order to adapt the new digital receiver to the existing radar system, a microwave printed circuit board was designed to convert the original 132.5 MHz IF to the required 25 MHz IF.

T/R tube technology was used as a receiver protector during the RICO. The TR tube has a limited operating life due to the interior radioactive gas decay. As the gas decays, the required energy to activate the device rises and the device produces a small amount of excess noise. The aged TR tube not only introduced unwanted noise into the receiver, it also exposed the receiver LNA to potential damage from the transmit pulse. A combination of an active ferrite switch cascaded with a diode limiter replaced the T/R tubes. Both devices combined provide more than 70 dB of isolation when activated. The recovery time is about 0.5 μs (150m blind range). An active ferrite switch directs transmit leakage to a high power termination and opens the path during receive mode. The replacement of the receiver protector has improved system noise figure by 1.7 dB.

Real-time status monitoring was established and integrated into a GUI. This mechanism assists the radar engineer to monitor the stability of the system. Various temperature sensors were installed throughout the system to provide warnings in the event of excessive heat. Oscillator lock status and programmable frequency information are also monitored. Operators are able to view status of the transmit and receive systems in real-time from a single GUI during radar operation.

A fiber optic rotary joint was installed in S-PolKa pedestal to replace the 802.11b wireless link to the data archiver. The data transmission rate of 10MB/s enables recording Ka-band in-phase and quadrature time series information possible. Moments data are recorded in CFRadial format.

Table 1: SPolKa Ka-band radar system specification

Antenna Subsystem	
Type	Cassegrain
Diameter	0.7 m
Gain	45.9 dB
Beamwidth	0.93°
Transmitter and receiver subsystem	
Transmitter	
Type	Magnetron
Frequency	34.693 GHz
Peak Power	50 kW
Pulse Width	0.5 μs
PRF	1 kHz
Receiver	
Noise Figure	5.28 dB
Dynamic Range	76.4 dB
Receiver Bandwidth	10 MHz
Sensitivity	-20.3 dBZ@10km, 0dB SNR

3. System performance

Ka-band performance was evaluated upon completion of the upgrade. The gain of the receiver channels was

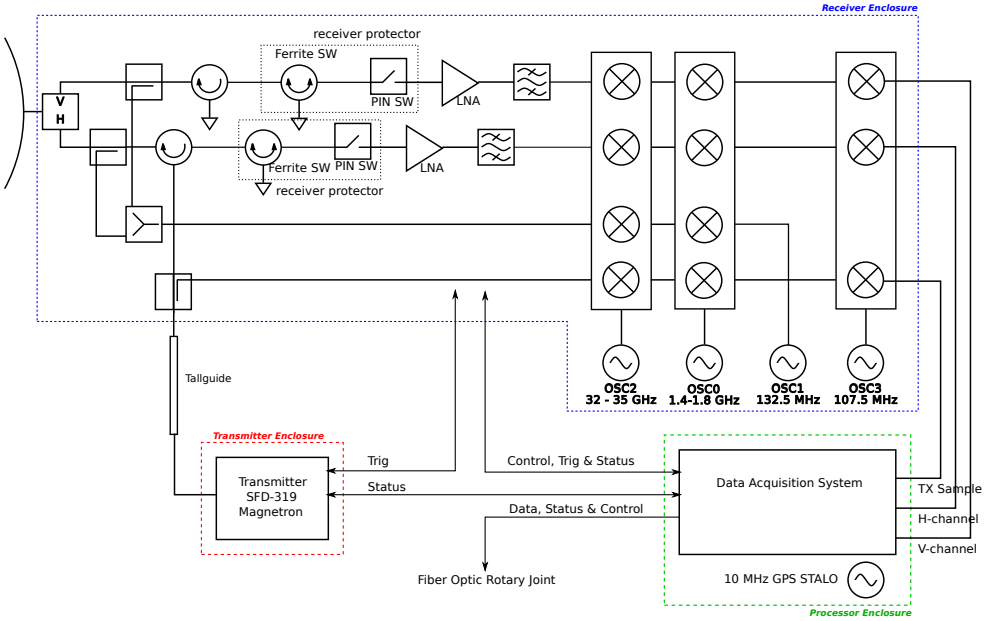

Figure 2: A Simplified block diagram of Ka-band radar system in LDR configuration.

measured to ensure maximum dynamic range. The dynamic range of receiver is 76 dB for both channels. System noise figure was derived from the Y-factor method. Measurements from noise source hot and cold settings were performed on both channels. Receiver noise figures are 5.3 dB and 6.1 dB for H and V channel respectively. The transmitter outputs 33 kW peak power at the antenna port. These improvements result in a minimum detectable signal of -103.25 dBm. This corresponds to a sensitivity of -20.3 dBZ at 10 km range.

4. Sample data

A preliminary data quality analysis of Ka-band radar measurements is presented in this section. S- and Ka-band radar measurements in stratiform rain were collected on April 19, 2011. The radar was located at the Marshall site near Boulder, Colorado. Figures 3 top and bottom show PPI images of refletivitiy at S- and Ka-bands respectively. At near range to the radar, S- and Ka-band reflectivities are of the same value. The Ka-band reflectivity is rapidly attenuated in the stratiform rain. Minimum reflectivity at 25 km range is -10 dBZ. This value is comparable to the expected sensitivity of Ka-band radar system.

Figure 4 shows RHI images of S-and Ka-band measurements. Figure 4a and 4b are S- and Ka-band reflectivity respectively. As expected low elevation scans through rain, Ka-band, reflectivity, is more attenuated than at high elevation scans through the frozen precipitation. Fine scale features in both S- and Ka-band are aligned. Precise alignment of S-band Ka-band radar measurements are critical for dual-wavelength analysis. Figures 4c and 4d show S- and Ka -band measurements of linear depolarization ratio (LDR). Both the S- and Ka-band measurements show bright band feature corresponding to the melting layer. Ka-band LDR is about 7 dB greater than than S-band LDR. In general Ka-band LDR will be higher than S-band LDR due to Mie scattering and attenuation. Fine scale features of LDR in S- and Ka-band measurements are aligned well. Detailed analysis of the Ka-band radar data quality will be conducted using the measurements from DYNAMO field deployment.

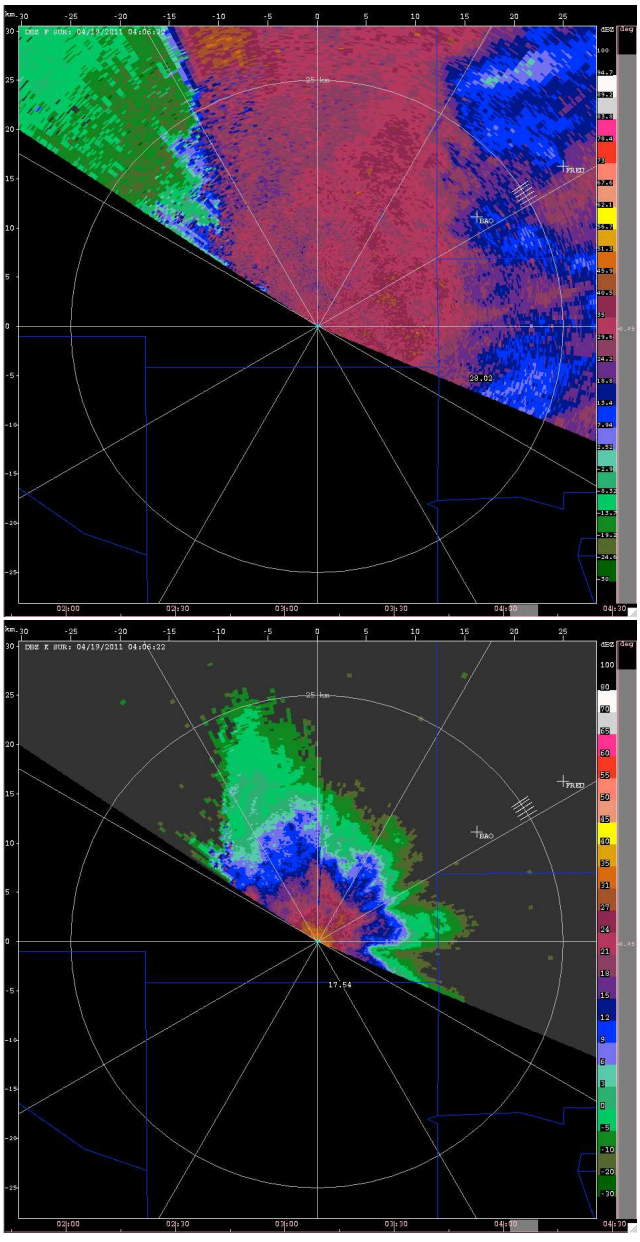

Figure 3: PPI images of reflectivitiy at S- (top)and Ka-band (bottom).

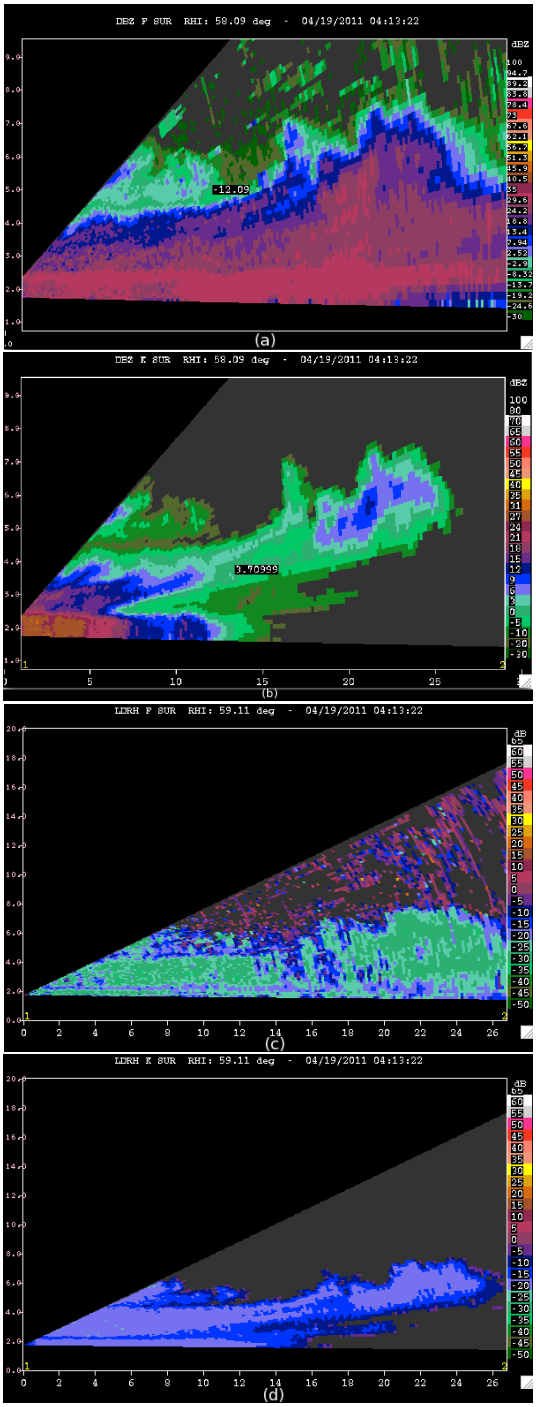

Figure 4: Reflectivity and linear depolarization ratio of S- and Ka-band RHI scans.

5. Summary

The Ka-band radar system of the S-Polka has undergone a significant upgrade in 2011. The new SFD-319 tube overcame the short life time of the transmitter. The new system could be operated unattended for extended periods, if desired. Overall sensitivity of the system has significantly improved as a result of stable frequency of operation, low loss T/R switch and a high-end digital processor. The system now has the capability to record time series data, as the fibre optic rotary joint offers higher data transmission rate. The radar is currently operational at the DYNAMO field deployment.

Acknowledgement The National Center for Atmospheric Research is sponsored by the National Science Foundation.

References

[1] F. Pratte, M. Pipersky, D. Ferraro, A. Phinney NCAR S-POL SECOND FREQUENCY (Ka-BAND) RADAR *Repr. fo 32st Conf. on Radar Meteorology*, AMS

[2] R.J., J. Lutz, and J. Vivekanandan S-Pol: NCAR's polarimetric Doppler research radar *Proceedings of the International Geoscience and Remote Sensing Symposium, IEEE, Honolulu, Hawaii 1570-1573*

[3] Ellis, S., K. Goodman, J. Vivekanandan, and C. Kessinger, 2005: Water vapor and liquid water estimates using simultaneous s and ka band radar measurements. *32nd Conf. on Radar Meteor.*, AMS.